Journal Pre-proof

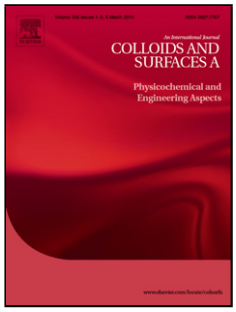

Chitosan/Heparin Polyelectrolyte Complexes as ion-paring approach to encapsulate Heparin in orally administrable SLN: in vitro evaluation

Eleonora Maretti (Methodology) (Project administration), Barbara Pavan<ce:contributor-role>Metodology) (Data curation), Cecilia Rustichelli<ce:contributor-role>Metodology) (Data curation), Monica Montanari (Investigation)<ce:contributor-role>validation), Alessandro Dalpiaz (Writing - original draft), Valentina Iannuccelli (Writing - review and editing), Eliana Leo (Conceptualization) (Funding acquisition) (Supervision)

PII: S0927-7757(20)31199-7

DOI: https://doi.org/10.1016/j.colsurfa.2020.125606

Reference: COLSUA 125606

To appear in: *Colloids and Surfaces A: Physicochemical and Engineering Aspects*

Received Date: 3 June 2020

Revised Date: 14 September 2020

Accepted Date: 16 September 2020

Please cite this article as: Maretti E, Pavan B, Rustichelli C, Montanari M, Dalpiaz A, Iannuccelli V, Leo E, Chitosan/Heparin Polyelectrolyte Complexes as ion-paring approach to encapsulate Heparin in orally administrable SLN: in vitro evaluation, *Colloids and Surfaces A: Physicochemical and Engineering Aspects* (2020), doi: https://doi.org/10.1016/j.colsurfa.2020.125606

Chitosan/Heparin Polyelectrolyte Complexes as ion-paring approach to encapsulate Heparin in orally administrable SLN: in vitro evaluation

Eleonora Maretti[a], Barbara Pavan[b], Cecilia Rustichelli[a]. Monica Montanari[c], Alessandro Dalpiaz[d], Valentina Iannuccelli[a], Eliana Leo[a,*]

[a]Department of Life Sciences, University of Modena and Reggio Emilia, via Campi, 103, 41125, Modena, Italy.

[b]Department of Biomedical and Specialist Surgical Sciences, University of Ferrara, via L. Borsari 46, 44121, Ferrara, Italy.

[c]Department of Life Sciences, University of Modena and Reggio Emilia, via Campi, 287, 41125, Modena, Italy.

[d]Department of Chemical and Pharmaceutical Sciences, University of Ferrara, via Fossato di Mortara 17/19, 44121, Ferrara, Italy.

*Corresponding author:

Eliana Leo, Department of Life Sciences, University of Modena and Reggio Emilia, via G. Campi 103, 41125 Modena, Italy tel. +39 059 2058558 *e-mail address*: eliana.leo@unimore.it

Graphical abstract

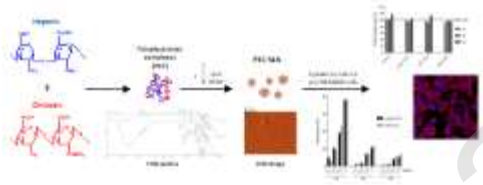

Highlights

- "Lipidization" of drugs by SLN encapsulation enhances their GI absorption
- Chitosan/heparin complexes allow heparin encapsulation in SLN
- Hybrid PEC-SLN displayed suitable size and pH controlled release
- Caco2 internalization of PEC-SLN were rapid and not time-dependent
- Chitosan inside SLN-PEC does not altered the integrity of tight junctions

ABSTRACT

Enhancing oral bioavailability of hydrophilic drugs by encapsulation in lipid-based nanocarriers, including Solid Lipid Nanoparticles (SLN), has been well documented. In this work, high molecular

weight heparin was “insolubilized” by an “ion-paring” approach, forming Chitosan/Heparin Polyelectrolyte Complexes (PEC) to promote its encapsulation in SLN. Hybrid PEC-SLN, heparin-loaded SLN (H-SLN) as well as naked PEC were prepared and characterized regarding size, Z potential, morphology, drug loading and drug release. Physicochemical characterization of the nanoparticles was also performed by differential scanning calorimetry (DSC), and Fourier Transform Infra-Red (FTIR) analysis. FITC-labeled naked PEC along with Nile Red labeled PEC-SLN were assessed on CaCo-2 cells to study cytotoxicity as well as cell internalization ability by cytometric and confocal analysis. Transepithelial electrical resistance (TEER) was measured on NCM460 cell monolayers to evaluate whether chitosan may induce a modification of tight junctions’ integrity at epithelial level. Results showed that the minimum size of PEC (around 170 nm) was at pH 5.5 with a positive surface charge and after encapsulation in SLN produced hybrid PEC-SLN with a size of about 370 nm and a negative zeta potential. In comparison to both H-SLN and naked PEC, PEC-SLN were able to achieve a pH-controlled drug release and showed on CaCo-2 cells low toxicity and rapid internalization. Finally, TEER measurements highlighted that the hybrid nanocarriers were internalized without interference in the membrane resistance. Therefore, PEC-SLN could be considered valuable candidate for further *in vivo* investigations about the systemic bioavailability of oral heparin.

KEY WORDS , lipid-based nanoparticles, TEER, DSC, CaCo2 cells, NCM460 cells

1. Introduction

Lipid-based colloidal systems currently constitute versatile technological platform in therapeutic and nutraceutical research fields for the design of innovative oral formulations of active ingredients. The improvement of the oral bioavailability through the use of lipid-based formulations, including emulsions, micellar systems, self-emulsifying drug delivery systems, liposomes and Solid Lipid Nanoparticles (SLN), is well documented [1,2]. In particular, these nanocarriers have been applied

successfully for drugs suffering of poor solubility, insufficient bioavailability and stability issues [3]. Among the lipid-based nanosystems, SLN have drawn particular attention owing to their submicron size, ease of scale up and manufacturing, use of physiological lipids and controlled release properties [4,5]. Moreover, SLN ranging from 50 to 1000 nm have shown the ability to improve transport via intestinal epithelial layer and their internalization is mediated by macropinocytosis pathway and clathrin- and caveolae (or lipid raft)-related routes [6]. Moreover smaller sized particles can be efficiently taken up by lymphoid tissues, where they bypass the first pass metabolism and increase bioavailability of the loaded drug [7].These properties of SLN can be exploited for the oral transport of biomolecules such as heparins (at high or low molecular weight) which are associated to invasive administration routes [8]. Due to their fragility towards physiologic obstacles such as in gastrointestinal (GI) tract, where they are quickly degraded before absorption, these molecules are currently administered via parenteral route [9,10]. New generation oral anticoagulants appear greatly promising in treating orally venous thromboembolism (VTE), but bleeding risk and chemotherapeutic drug interactions are still serious clinical constraints for this type of drugs. The development of orally administered active anti-thrombotic agents, such as heparins, can be therefore useful in the clinical use in order to avoid long-term subcutaneous injection during follow-up medication after discharge from hospital or during both treatment and prevention of chronic diseases. Moreover, innovative oral formulations for heparin are currently required, taking into account that orally administered heparins are considered a promising tool inducing effective suppression of cancer-associated thrombosis (CAT) [11,12], i.e. thromboembolic events, including deep-vein thrombosis (DVT) and pulmonary embolism (PE), that significantly contribute to lead cancer patients to death [13].

In the aim to achieve oral administration, the “lipidization” of hydrophilic biomacromolecules has proven to enhance their hydrophobicity and hence the GI absorption possibility [14]. Several conjugates between lipids or steroids and low molecular weight heparin (LMWH) have been previously developed and evaluated for its oral bioavailability enhancement [8,12,15]. The use of SLNs can be considered very promising since SLNs are considered enhancers for the intestinal

absorption of poorly absorbable drugs [16]. However, for its hydrophilicity, direct incorporation of heparin into SLNs will result in very low encapsulation efficiency and drug loading owing to the rapid migration of the drug towards the particles' surface during the solidification of the melted lipid [17]. The strategies adopted to solve this problem are poor, and the one reported is by chemical modification of the molecule by lipid conjugation [9,12].

In the present study, in order to avoid chemical conjugation, high molecular weight heparin was water "insolubilized" by an "ion-paring" approach, suppressing its negative charge by coupling with chitosan, a polymer widely used as an oral absorption enhancer [18]. In this aim, Chitosan/Heparin Polyelectrolyte Complexes (PEC) were developed to facilitate the incorporation of heparin in SLN, obtaining PEC-SLN hybrid system. Hence, naked PEC, PEC-loaded SLN (PEC-SLN) as well as heparin-loaded SLN (H-SLN) were formulated and their physicochemical properties were compared to each other. Moreover, Fluorescein IsoThioCyanate (FITC) labeled PEC, along with Nile Red labeled PEC-SLN and empty SLN were incubated with CaCo-2 cell line to quantify their cytotoxicity and to study their internalization in the cells by cytometric and confocal analysis. Finally, transepithelial electrical resistance (TEER) was measured on a human established normal colon mucosa derived cell line (NCM460 cells) in order to evaluate the effect of this hybrid colloidal system on the integrity of intestinal tight junctions.

2. Materials and methods

2.1. Materials

For SLN preparation, Compritol 888ATO (glycerol behenate) was a kind gift from Gattefossè (Weil am Rhein, Germany), heparin sodium salt (167 U.I. /mg, MW 6-25 kDa,) from Biofer (Modena, Italy), Span 85 (sorbitan trioleate), Azure II, Nile Red from Sigma-Aldrich Italia (Milan, Italy),

Tween 80 (polysorbate 80), Fluorescein IsoThioCyanate (FITC) and chitosan (70 kDa; 75-85% deacetylated) from Fluka Chemie (Buchs, Switzerland) were purchased.

For the cell culture DMEM (Dulbecco's Modification of Eagle's Medium) with high glucose, L-glutamine, Fetal Bovine Serum (FBS), Penicillin-Streptomycin (P/S), Phosphate Buffer Saline (PBS) and Trypsin 2.5% in HBSS were purchased from EuroClone and Lonza Italia (Milan, Italy).

All the other chemicals were of analytical grade.

2.2. Preparation and characterization of Chitosan/Heparin Polyelectrolyte Complexes

Chitosan/Heparin Polyelectrolyte Complexes (PEC) were prepared by self-assembly chitosan and heparin, according to the method proposed by Lin et al. (2009). Briefly, heparin, dissolved in deionized water (4 mL, 2 mg/mL), was added under magnetic stirring to a chitosan solution obtained by dissolving chitosan in 0.25% v/v acetic acid (25 mL, 0.5 mg/mL). The pH was adjusted to 5.5 with 1 N NaOH and the system was incubated for 30 min at room temperature. All experiments were performed in triplicate. Freshly prepared PEC was recovered by centrifugation at 16,000g for 1 h at 4°C (Rotina 380R, Hettich, Germany) before its incorporation in SLN.

To evaluate the non-complexed heparin after PEC formation, the amount of heparin was determined in the supernatant by using the colorimetric method based on the Azure II dye [19]. Typically, aliquots (500 µL) of aqueous phase (supernatant) were reacted with 4.5 mL of the Azure II solution (0.01 mg/mL) and assayed in triplicate at 654 nm by UV spectroscopy (Lambda 35 UV/VIS, Perkin-Elmer, Norwalk, CT, USA).

Naked PEC mean size (Z average) and polydispersity index (PDI) at different pH (from 1 to 9.2) were determined by Photon Correlation Spectroscopy (PCS) by a Malvern Zetasizer version 6.12, (Malvern Instruments, Worcs, U.K.) equipped with a 4mW He-Ne laser (633 nm) and a DTS software (Version 5.0). The zeta potential measurements were carried out using the Malvern Zetasizer by electrophoretic laser doppler anemometry at 25°C.

2.3. Synthesis of FITC-labeled chitosan

FITC-labeled chitosan was synthesized according to the method reported in literature [20]. Practically, 5 mL of methanol followed by 2.5 mL of FITC in methanol (2 mg/mL) was added to 5 mL of chitosan (1% w/v in 0.1 N CH_3COOH). The reaction was run for 3h in the dark at room temperature. Then, the labeled polymer was precipitated in 0.5 M NaOH at pH 10. The precipitate was recovered by centrifugation at 25,000g (10 min) (Mikro 120, Hettich Zentrifugen, Germany) and washed in a methanol/water mixture (70:30 v/v). The washing and the palletization were repeated until no fluorescence was detected in the supernatant. The labeled chitosan was then dissolved in 0.1 N CH_3COOH and dialyzed in the dark against deionized water for 3 days. Finally, the FITC-labeled chitosan was freeze-dried (Lyovac GT2, Leybold-Heraues GmbH, Koln, Germany) and stored at room temperature at dark. Labeled PEC for cell internalization experiments were obtained by adding FITC labeled-chitosan (5% w/w) to the acetic acid chitosan solution (0.5 mg/mL final chitosan concentration).

2.4. Preparation and characterization of SLN

To prepare SLN, a modified double emulsion method was used [21]. Briefly, all PEC pellets recovered by centrifugation (for PEC-SLN) or free heparin (7 mg) (for H-SLN) were dispersed in 0.3 mL of deionized water and emulsified at 70°C by ultrasounds with the melted lipid phase of Compritol ATO888 (0.5 g) and Span 85 (0.15 g). Then, 15 mL of an aqueous solution of Tween 80 (2%, w/v), kept at the same temperature (70°C), was poured in the previous emulsion and emulsified firstly by ultrasound, (130 W for 1 min) (Vibra-Cell, Sonics & Materials, Newtown, CT, USA), then by ultraturrax (24,000 rpm for 2 min) (Ika-euroturrax T 25 basic, IkaLabortechnik, Staufen, Germany). At the end, the system was rapidly cooled in ice under magnetic stirring and the obtained dispersion of SLN was purified once with a carbonate buffer solution pH 9.2 and twice with water by

diafiltration (PALL Macrosep® Advance Centrifugal Devices, 30KDa MCWO) at 2,600g for 30 min each wash (Rotina 380R, Hettich, Germany) to remove the excess of surfactant and the not-incorporated drug. Then, all the samples were freeze-dried without cryoprotectants at –55°C at a pressure of 10^{-4} Torr during 36h (Lyovac GT2, Leybold-Heraues GmbH, Koln, Germany) and the powder kept at 4°C at the dark. Labeled SLN for cell internalization were obtained by adding Nile Red (0.01%) to the melted Compritol.

Size, polydispersity index (PDI) and zeta potential were measured by using PCS equipped with a 4mW He-Ne laser (633 nm) and a DTS software (Version 5.0). The samples were evaluated both as soon as prepared and after freeze-drying. The re-dispersion of the freeze-dried samples (10 mg) was performed in deionized water (2 mL) by three cycles of vortex (30 cm) followed by a treatment in an ultrasound bath (Sonorex™, Bandelin, Mörfelden, Wan, Germany) (30 sec).

2.5. Morphological characteristics

Morphological characteristics of naked PEC and PEC-SLN were observed by a Park Autoprobe Atomic Force Microscope (Park Instruments, Sunnyvale, CA, USA). AFM images were obtained by measurement of the interaction forces between the tip and the sample surface. The experiments were conducted in water at room temperature (20 °C) and at atmospheric pressure (760 mmHg) operating in non-contact mode (NC-AFM). Triangular silicon tips were used for this analysis. The resonant frequencies of this cantilever were found to be about 120 KHz. Immediately before the analysis, the samples were diluted in water (1:100 v/v) to obtain a less sticky fluid and deposited (40 µl) onto a small mica disk with a diameter of 1 cm. After 2 min, the excess of water was removed using paper filter. *2.6. DSC and FTIR analyses*

Fourier Transform Infra-Red (FTIR) spectra were recorded on PEC and SLN as well as on their single components by Attenuated Total Reflectance (ATR) at 35 °C (FTIR Vertex 70, Bruker, Optics – Ettlingen, Germany).

Thermograms on SLN, single components and physical mixture of Compritol and heparin were recorded by differential scanning calorimeter (DSC) (DSC-4, Perkin- Elmer, Norwalk, CT, USA) previously calibrated with indium. Heating rate of 20°C/min was employed over a temperature range of 30–350 °C with nitrogen purging (30 mL/min). The physical mixture of Compritol and heparin was prepared using the same lipid/drug ratio as SLN. Moreover, Compritol and physical mixture were pre-heated in accordance to temperature conditions used for the SLN preparation before DSC analysis.

2.7. Drug loading, encapsulation efficiency and in vitro release

The determination of the heparin loaded in H-SLN and PEC-SLN was performed by using the colorimetric method based on the Azure II dye [19]. An aliquot of freeze-dried SLN (10 mg*)* was dissolved in 1 mL of chloroform; then 3 mL of deionized water or carbonate buffer solution pH 9.2 was added for H-SLN or PEC-SLN, respectively. Heparin was determined in the aqueous solution by the colorimetric assay. Typically, aliquots (500 µl) of aqueous phase were reacted with 4.5 mL of the Azure II solution (0.01 mg/mL) and assayed in triplicate at 654 nm by UV spectroscopy. Drug loading (DL) and encapsulation efficiency (EE) values are averaged on three determinations and calculated as follows

$$\text{DL (\%)} = \frac{mass\ of\ drug\ in\ SLN\ (mg)}{mass\ of\ SLN\ powder\ freeze\ dryed\ (mg)}\ \text{x } 100 \qquad (1)$$

$$\text{EE (\%)} = \frac{entrapped\ amount\ of\ drug\ per\ g\ nanoparticles}{theoretical\ amount\ of\ drug\ per\ g\ nanoparticles}\ \text{x } 100 \qquad (2)$$

Heparin *in vitro* release studies were performed by incubating at 37 °C PEC-SLN or H-SLN (50 mg) in HCl 0.1N (50 mL) at pH 1 (for the first 3h), then at pH 6.8 (for the followed 6h) and finally at pH

7.5 (followed 15h) in order to simulate the passage through gastrointestinal tract. At various time intervals, 0.5 mL samples were withdrawn and replaced with fresh solvent to maintain constant volume and filtered upon centrifugation at 13,000*g* using microcon filter devices (YM 100, Millipore Corporation, Bedford, MA, USA). The supernatant was removed and assayed for heparin according to the Azure II colorimetric method.

2.8. Cell cultures

CaCo-2 cell line was cultured in Dulbecco's Modified Eagle Medium (DMEM) containing 2 mM L-glutamine, 100 U/mL penicillin, 100 µg/mL streptomycin and 10% Fetal Bovine Serum (FBS) at 37ºC in a humidified 5% CO_2 atmosphere. Cells were subcultured when the confluence was ≥ 80%. NCM460 cells, an established cell line derived from human normal cell colon mucosa, were grown in DMEM medium supplemented with 10% FBS, 100 U/mL penicillin and 100 µg/mL streptomycin at 37°C in a 95% humidified atmosphere, with 5% CO_2. For optimal viability, subculture of NCM460 cells was done in fresh and spent medium in 1:1 ratio.

Labeled samples were used in all the *in vitro* cell experiments as following indicated: naked PEC labeled with FITC, PEC-SLN and empty-SLN labeled with Nile Red.

2.8.1. Cytotoxicity assay on CaCo-2 cells

Naked PEC, PEC-SLN and empty-SLN were assayed *in vitro* on CaCo-2 cells in order to evaluate their cytotoxicity by MTT test. Cells were seeded at a density of 75,000 cells/well in 24-well plate in complete DMEM's medium for 48h at 37°C with 5% CO_2. Then, cells were incubated in complete medium for 4, 6 and 12h with 0.2, 0.4, 0.8 and 1.2 mg/mL SLN (PEC-SLN and empty-SLN; suspensions were obtained by vortex mixing for 2 min and sonic bath at 37 °C for 1 min) or with naked PEC amounts equivalent to those encapsulated in SLN (15, 30, 60 and 90 µg/mL, respectively).

100µl of a 0.5 mg/mL MTT solution were added to each well at the programmed time points. After 1h of incubation the medium was removed, the well was washed with PBS and 1 mL of dimethyl sulfoxide (DMSO) was added to each well. Optical densities were measured spectrophotometrically at a wavelength of 570 nm. Cell viability was expressed as a percentage of cell growth with respect to the control (untreated cells).

2.8.2. Nanoparticles internalization in CaCo-2 cells

Labeled nanoparticles (PEC-SLN and empty-SLN) and naked PEC, were tested for their ability to be taken up by CaCo-2 cell line. Cells were plated in 6-well plates (200,000 cells per well) and incubated for 4, 6 and 12h with 0.2, 0.4, 0.8 and 1.2 mg/mL SLN suspensions or with naked PEC amounts equivalent to those encapsulated in SLN (15, 30, 60 and 90 µg/mL, respectively).

Cells were washed twice with PBS at each time point and then detached with trypsin and collected for flow cytometric analysis. Flow-cytometry evaluation of intracellular uptake was performed by a COULTER® EPICS® XL™ (Beckman Coulter Inc., 250 S. Kraemer Blvd, Brea, CA 92821, US) flow cytometer equipped with a 488 nm argon laser. Fluorescent cells with Nile Red or FITC were expressed as a percentage of the total cell population. The experiments were performed in duplicate.

2.8.3. Transepithelial electrical resistance (TEER) measurements on NCM460 cells

For the measurements of transepithelial electrical resistance (TEER), NCM460 cells were seeded at density of 50×10^4 cells/insert (1.5×10^5 cells/cm^2) in the complete medium onto polyethylene terephthalate (PET) filter 24-wells ThinCerts™ inserts, with the membrane pore size of 1 µm and 0.33 cm^2 surface. In particular, the filters were pre-soaked for 24h with the complete medium and then the upper compartment (apical, A) received 0.2 mL of the diluted cells, whereas the lower (basolateral, B) received 1.25 mL of the complete medium. Cells were fed with fresh growth medium

every 2-3 days and confluent polarized monolayers were obtained 6 days after plating. At this time, the growth medium was changed with low serum (1% FBS) DMEM fresh medium on both the basolateral and apical side and integrity of cell monolayers was determined by TEER measurements, using a voltmeter (Millicell-ERS; Millipore, Milan, Italy) equipped with chopstick electrodes.

TEER was expressed as $\Omega \cdot cm^2$ and calculated as (Total resistance - Background resistance) (Ω) × Area (cm^2 monolayer). The background resistance of blank inserts was about 35 $\Omega \cdot cm^2$. Monolayers with TEER stable value around 180 $\Omega \cdot cm^2$ were used for cell monolayer tightness studies. In particular, the apical compartments received 0.4 mg/mL SLN samples or 30 µg/mL naked PEC, then TEER values of cell monolayers were measured after incubation for 2, 4 and 6h.

2.8.4. Confocal microscopy study on CaCo-2 and NCM460 cell lines

For multi-channel fluorescence co-localization by confocal microscopy, NCM460 cell monolayer (grown on ThinCerts™) and CaCo 2 cells were observed after 4h of incubation with 0.4 mg/mL PEC-SLN, empty-SLN and naked PEC (30 µg/mL). The cells were fixed in paraformaldehyde (3%, w/v) for 20 min at room temperature and observed under filter set for red and green fluorescence by using confocal laser scanning microscopy (CLSM; DM IRE2, Leica Microsystems, Heidelberg, Germany) at 1.1 µm step after cell nucleus staining by Hoechst 33258 stain (blue) (2 µg/mL) for 20 min at room temperature.

2.9. Statistical analysis

Statistical analysis was performed using the one-way analysis of variance (ANOVA). The data are represented as means ± SD. Differences were considered statistically significant at p values less than 0.05.

3. Results and discussion

3.1. PEC formation and characterization

The oral route has been always considered the most convenient and preferred administration way for drugs. In this work, lipid-based nanosystems have been designed and formulated for heparin oral delivery. Among the various interesting nanoformulations known in literature to attain oral bioavailability of drugs with poor gastro-intestinal absorption, SLN seem to have an important role in enhancing biomacromolecules bioavailability [16], even if, currently, the exact mechanism by which nanostructurated lipids enhance intestinal absorption has not yet been clarified [7]. In this work, Chitosan/Heparin Polyelectrolyte Complexes (PEC) formation has been chosen as a strategy to improve/allow the incorporation of a water-soluble molecule, such as heparin, into a lipid core composed by selected materials, safe and approved by the FDA for oral administration.

PEC obtained by ion paring mechanism were prepared in order to reduce heparin water solubility thus improving its encapsulation in SLN. Fig 1 reports FTIR spectra of chitosan, heparin, and PEC. PEC spectrum exhibited the characteristic main bands of the two precursor components. The occurred complexation is indicated by the bands at 1632 and 1535 cm^{-1} attributable to the amide bonds between the amine group and the carboxylic group of chitosan and heparin, respectively. Moreover, the band

related to sulfate groups, which occurred in heparin spectrum at 1224.1 cm^{-1}, shifted in PEC spectrum at 1215 cm^{-1} probably due to the ionic interaction [22].

For PEC formation, both polymers have to be ionized with opposite charges [23], therefore, the best pH values allowing successful PEC making range between the two pKa of the polymers (3.1 and 6.5 for heparin and chitosan, respectively). Indeed, as reported in Table I, PEC size is dependent on the pH of the medium. In particular, PEC are stable in acidic medium where chitosan can be highly positively charged together with negatively charged heparin and this facilitates the formation of compact complex with relatively small size. On the other hand, in approximately neutral conditions (pH 6.8) an increase in their size occurred, while in basic condition the system became instable leading to formation of precipitates. Indeed, in this pH range the interaction between polymers are practically inexistent.

As reported in Table I, the most suitable pH for PEC formation resulted 5.5 confirmed by AFM analysis were complexes appeared spherical in shape ranging between 100 and 200 nm with homogeneous size distribution (Fig. 2A). It is important to underline that PEC analysis by AFM revealed particle sizes smaller than those measured by PCS (Table I). This difference is probably due to the dissimilar environmental conditions involving the two techniques during size measurements of the nanoparticles. Indeed, during PCS analysis nanoparticles were suspended in aqueous medium, so the nanocomplexes were well swelled, while for AFM measurements, PEC was previously shrink under drying. Similar phenomena have been reported previously [24].

After complex formation at pH 5.5, PEC were recovered by centrifugation and non-complexed heparin was quantified in the supernatant. A small amount of heparin (about 5% of the original amount) was detected indicating that, at this pH condition, 95% of heparin (corresponding to about 7.5 mg) was complexed with chitosan forming PEC.

3.2. SLN formulation and physicochemical characterization

PEC pellet was encapsulated in SLN in order to formulate PEC-loaded SLN (PEC-SLN). Moreover, also unloaded SLN (empty-SLN) and heparin loaded SLN (H-SLN) were obtained. All the nanoparticles were characterized about their size, polydispersity index (PDI) and zeta potential before and after freeze-drying (Table II). The measurements were performed on both fresh and reconstituted freeze-dried samples.

Considering fresh samples, the mean diameter of empty-SLN was about 200 nm with homogeneous size distributions (PDI<0.3) while H-SLN and PEC-SLN showed larger particle size up to about 350 nm without changes in the size distribution. All SLN exhibited negative zeta potential in the range of -23 to -10 mV and the less negative value, -10.3 mV, was observed for PEC-SLN, probably due to the shielding of positively charged PEC on the particle surface. To ensure long-term stability of liable pharmaceuticals and in order to handle these delivery systems in the form of dry state, freeze-drying process can be considered an excellent method compared to other drying techniques [25]. Freeze-drying was obtained in the absence of cryoprotectants to avoid cell permeability alteration during *in vitro* tests [26]. Freeze-dried SLN were reconstituted and evaluated for their physicochemical characteristics in comparison to the freshly prepared samples (Table II).

Reconstituted freeze-dried samples shown a slight increase in size and PDI values ($p<0.05$), probably due to the presence of small percentage of aggregates, while zeta potential remained unchanged compared to fresh samples ($p>0.05$). Based on these data, being PDI ranged between 0.293 - 0.419, all these nanocarriers can be considered re-dispersible after freeze-drying.

To further investigate the nanostructural characteristics of PEC-SLN, the lyophilized sample was examined by AFM (Fig. 2A). AFM analysis demonstrated spherical particles of about 200-400 nm in diameter along with few aggregates. The outcome, as well as for H-SLN (Fig. 2A), is roughly in agreement with particle size measurements using PCS.

Moreover, pre-heated Compritol, pre-heated physical mixture of Compritol and heparin, and SLN samples have been analyzed by DSC (Fig. 1S, 2S, and 3S in Supplementary Material). Table III shows the change of melting temperature (Tm) and enthalpy (ΔHm) values for Compritol in the different

samples. The endothermic event in pre-heated Compritol and pre-heated physical mixture at 74.06 °C and 75.65 °C, respectively, represents the melting peak of the metastable polymorphic forms of the lipids of which Compritol is composed (mixture of mono-, di- and triacylglycerols); moreover, slightly different values of melting enthalpy were observed namely 128.91 and 124.64 J/g for Compritol and physical mixture, respectively. In the thermogram of physical mixture, endothermic events attributable to heparin are not visible probably owing to its low amount.

Empty-SLN thermogram showed the melting peak related to Compritol at a temperature lower than that of pre-heated Compritol and pre-heated physical mixture (~ 71°C with respect to ~ 74 or ~ 75°C), probably due to the effect of the smallest size of particles [27]. Moreover, the lower melting enthalpy suggests a minor crystallinity, that may be induced by the presence of surfactants and by the freeze-drying process [27,28]. Comparing thermograms of empty-SLN, H-SLN and PEC-SLN, a gradual reduction in melting temperature and enthalpy values was observed in the following order: empty-SLN> H-SLN > PEC-SLN (Table III), being more evident in PEC-SLN. The encapsulation of drug may exert an important role in determining this phenomenon since it is reported that the presence of a drug in a lipid matrix can generate disturbance of the lipid crystal order [29,30]. Therefore, this finding indicates the incorporation of the drug in the lipid matrix as both free molecule (in H-SLN) and polyelectrolyte complex (in PEC-SLN).

On the other hand, despite having conducted FTIR analyses on all samples tested with DSC, FTIR spectra do not provide additional information on the encapsulation process as the drug band was not visible in any case, including the physical mixture, given the low concentration of drug in the lipid matrix (Fig. 4S and 5S in Supplementary Materials).

3.3. Determination of heparin loading in H-SLN and PEC-SLN

Since a high-energy method was used to produce SLN, before the purification step, the amount of heparin was determined in both PEC-SLN and H-SLN suspensions to verify if heparin was detectable

after the encapsulation process or, in other words, if heparin was degraded during the formulation processes. Chloroform was added to the suspensions in order to dissolve SLN and heparin was measured in the dispersed phases with the colorimetric method. Table IV shows that the SLN formulation process did not significantly change the heparin amounts detected in the suspensions, with respect to its original values.After preparation, SLN samples were purified by diafiltration and then freeze-dried. Heparin loading and encapsulation efficiency in freeze-dried SLN is reported in Table IV. Data show that drug loading as well as encapsulation efficiency is slightly higher in the case of H-SLN compared to PEC-SLN. Therefore, according to loading data, the encapsulation efficiency of heparin into the SLN does not seemed to be improved by the use of PEC systems, despite they provided reduction of the heparin water solubility, with respect to the free drug.

However, these data do not indicate whether the drug is actually incorporated into the nanoparticulate systems or only adsorbed on their surface. In order to check the effective incorporation of the drug, *in vitro* release experiments were conducted in simulated gastro-intestinal medium.

3.4. In vitro release of heparin from naked PEC, PEC-SLN and H-SLN

To verify the ability of the SLN in modulating heparin release into the gastro-intestinal tract, the experiments were performed in simulated gastric (pH 1), intestinal pH (pH 6.8) and in physiological environment (pH 7.5) over a time interval of 24h, progressively varying the pH. The analysis was also conducted on naked PEC, as a control. Data in Fig. 2B clearly evidence that H-SLN sample rapidly released heparin during the first minutes in acidic environment. This result suggests that the drug is incorporated close to the surface of the particles . Probably, during the formation of the particles, heparin given its high-water solubility diffused into the external aqueous phase remaining mostly encapsulated in the outermost layers of the particles . On the other hand, heparin release from PEC-SLN, appeared pH modulated. In particular, at pH 1 heparin release was negligible as well as in the case of naked PEC. This result can be explained considering that at these pH conditions PEC was

characterized by good stability, as previously evidenced. It is known that at pH 6.8 the electrostatic interactions between chitosan and heparin markedly decrease and become negligible at physiological conditions (pH 7.5) [23,24]. Indeed, at these pH conditions heparin was rapidly released from naked PEC (Fig. 2B). PEC-SLN sample, instead, produced at pH 6.8 only a slight burst (about 17%), as evidenced in Fig. 2B, probably due to the PEC adsorbed on the surface of the particles, then, a steady state until the end of the analysis time interval was observed. This pattern indicates a good ability of PEC-SLN to control the heparin release in all the pH condition of the intestinal tract. Therefore, according to these results it can be hypothesized that heparin is protected in SLN along the first stretch of the gastro-intestinal tract and starts to be released only in the small intestine where the highest extent of intestinal absorption occurred.

On the basis of the release results, *in vitro* assays on biological systems were performed only with PEC-SLN, using empty-SLN and naked PEC as controls.

3.5. In vitro study on CaCo2 cells

CaCo-2 cells, an immortalized cell line derived from human epithelial colorectal adenocarcinoma, have been wildly accepted as an *in vitro* model of small intestine in the studies of formulations designed for oral drug administration. [31,32]. Whereas the biocompatibility of drug carriers is a major issue in their developing [33,34], in the case of oral route, the assessment of any potential toxic interaction with intestinal epithelia appears as a crucial aspect. Therefore, to evaluate cell cytotoxicity on CaCo-2 cell line, the metabolic assay MTT was used [35]. The cytotoxicity of PEC-SLN and empty-SLN was estimated using increasing dose from 0.2 to 1.2 mg/mL after 4, 6 and 12h of exposure.

After 4h of incubation, a slight cellular toxicity no dose-dependent was observed for all the samples at the tested doses (Fig. 3). The average cell viability was between 65 and 75%, indicating that these doses were lower than DL50. Empty-SLN induced, on cells treated after 6h incubation, a weak dose-

dependent effect, differently from PEC-SLN. It is worth noting that at this time point the cytotoxicity of all the samples resulted lower than that detected at 4 h. This trend was confirmed after 12h when PEC-SLN resulted no cytotoxic and only a slight dose-depended toxicity was evidenced for empty-SLN. The cells were also incubated with naked PEC amounts ranging between 10 and 90 µg/mL. These amounts were equivalent to those encapsulated in PEC-SLN and produced the same trend observed for loaded SLN (Fig.3).

The overall viability data suggest a time dependence but not a dose dependence of the toxicity induced by all the analyzed samples toward CaCo-2 cells. Surprisingly, toxicity tended to decrease with the increase of the incubation time, particularly in the case of PEC-SLN and naked PEC, probably for the presence of chitosan acting as activator of cellular metabolism [36].

Flow cytometry results reported in Fig. 4 indicate that uptake of empty-SLN and PEC-SLN, for all the incubation times, was clearly dose-dependent, whereas the uptake of naked PEC was very low and not dose-dependent. After 4h treatment a large internalization was observed with empty-SLN and PEC-SLN but not with naked PEC. This result suggests the crucial role of SLN as a preferential carrier for cellular uptake into CaCo-2 cells. It is noteworthy that the overall decrease of the SLN internalized with the increase of the exposure time (from 4 to 12h) is in agreement with the data of toxicity which showed higher toxicity for short time of contact.

The peak of internalization observed after 4h is in agreement with the data reported in the literature as the maximum internalization of lipid nanoparticulate systems in CaCo-2 cells is recorded in a range of 1 to 4h [8,37]. Only few studies have evaluated in CaCo-2 longer internalization times, highlighting that cells could uptake more particles but the speed dropped gradually [38]. The intracellular fate of SLN into CaCo-2 cells has been deeply investigated. They will be transported from the apical membrane to cytoplasmatic organelles, such as Golgi apparatus and microtubules. These cellular organelles are responsible of SLN exocytosis via the apical or the basolateral membrane [6]. Therefore, the decrease in the fluorescence recorded in CaCo-2 cells with increasing incubation time

could be attributed to the exocytosis activity of cells highlighted in monolayers from the basolateral side but also observed from the apical side especially for non-polarized cells [6,39].

In order to clarify the localization in the cells of SLN and naked PEC, confocal microscopy was performed on CaCo-2 cells, having blue stained nuclei, incubated for 4h with Nile Red labeled PEC-SLN and FITC labeled naked PEC with a dose of 0.4 mg/mL and 30 µg/mL, respectively. Images reported in Fig. 5 indicate unequivocally that the localization of the particles (PEC-SLN) was around the nuclei (Fig. 5a) i.e. in the cell cytoplasm and not in the space between cells. At the same incubation time the amount of naked PEC (green fluorescence) around the nuclei was very poor (Fig. 5b), in accordance with the results obtained by flow cytometer.

3.6. Transepithelial electrical resistance (TEER) measurements

As chitosan is known to promote the opening of tight junctions [40], its presence in the samples induces to investigate whether, during the internalization process, a modification of the epithelial barrier integrity occurred. Therefore, measurement of TEER was carried out on cell monolayers of human normal colonic epithelial NCM460 cells during cell uptake of nanoparticles. NCM460 cell represent a non-transformed and non-tumorigenic cell line derived from primary cells of the normal human transverse colon mucosal epithelium [41]. After confluence in ThinCerts^{TM} inserts, cells acquire functional polarization forming a monolayer with epithelial barrier properties [42,43]. In particular, the TEER values of these monolayers appear closer to the range reported for intact sheets of human colonic mucosa than those developed by CaCo-2 cells [44,45], whose loss of contact inhibition and polarization in transformed cells is known to produce changes in growth characteristics (monolayers/multilayers) [46].

TEER measurements were performed by incubating the monolayers with 0.4 mg/mL of empty-SLN and PEC-SLN, and 30 µg/mL of naked PEC, since these doses showed significant internalization values in CaCo-2 cells. The TEER data detected at different time points are reported as percentage of

the initial value (time 0h, 185 ± 12 Ω · cm^2). Fig. 6A shows that no significant changes in TEER values were induced by the samples during the incubation time until 6h.

The sensitivity of this type of measurements, indeed, allows to consider significant the TEER changes when at least a drop of 50% with respect to control value occurs [47]. Since the TEER measurements were conducted on a cell line different from CaCo-2, in order to confirm the successful internalization of nanoparticles into NCM460 cell line, confocal analysis was carried out. Cells were incubated for 4h with PEC-SLN amounts corresponding to 0.4 mg/mL and then analyzed at confocal microscopy to verify the presence of particles into the cells. The images reported in Fig. 6B confirmed this assumption evidencing the massively internalization of the SLN in the cells.

Therefore, on the basis of these data, it can be stated that for all analyzed samples, including naked PEC, paracellular route arising *via* transient disruption of the tight junctions, does not occur [48]. About cellular internalization pathways, SLN can enter cells predominantly via the energy-dependent transport mechanisms of endocytosis [48–50]. On the basis of the TEER results, the SLN endocytosis, including PEC-SLN and naked PEC, does not involve the simultaneous opening of tight junctions mediated by chitosan. The inability of the chitosan containing-samples to open the tight junctions is probably due to functional groups of chitosan engaged in binding heparin in both PEC-SLN and naked PEC, making chitosan unable to exert any influence on the TEER values.

4. Conclusion

In this study "lipidization" of heparin has been accomplished by encapsulation of Heparin/Chitosan Polyelectrolyte Complexes (PEC) in SLN without chemical modification of the hydrophilic macromolecule. The encapsulation of PEC into SLN, instead of heparin in free form, allowed to obtain its pH-controlled release. The PEC-SLN systems show good potentialities for oral absorption evidenced by the release data, the low toxicity and the high internalization in CaCo-2 cells in relatively short times. The internalization mechanism is very controversial and difficult to define even

though many studies in the literature highlight that it does not occur by a single way but rather by concomitant mechanisms. Moreover, a study on a different cell line performed to assess the integrity of the junctions during the internalization process, allow us to conclude that the systems are internalized without interference in the membrane potential. Therefore, the lipid nanocarrier PEC-SLN could be considered valuable nanoparticulate systems to be further investigated about their ability to promote, *in vivo*, the oral bioavailability of heparin.

CRediT author statement

Eliana Leo: Conceptualization and Funding acquisition, **Eleonora Maretti** Methodology and Project administration, **Barbara Pavan and Cecilia Rustichelli**:Metodology and Data curation. **Alessandro Dalpiaz:** Writing and Original draft preparation. **Monica Montanari** Investigation and validation. **Valentina Iannuccelli***:* review & editing.: **Eliana Leo**: Supervision

Declaration of interests

The authors declare that they have no known competing financial interests or personal relationships that could have appeared to influence the work reported in this paper.

Acknowledgments

The authors are grateful to UniMoRE for the financial support (FAR-DSV 2019-Leo). Thanks are also due to Dr. Francesca Sacchetti and Dr. Raffaella Aracri for their valuable contribution to the work.

References

[1] Z. Niu, I. Conejos-Sánchez, B.T. Griffin, C.M. O'Driscoll, M.J. Alonso, Lipid-based nanocarriers for oral peptide delivery, Adv Drug Deliv Rev. 106 (2016) 337–354. https://doi.org/10.1016/j.addr.2016.04.001.

[2] O.M. Feeney, M.F. Crum, C.L. McEvoy, N.L. Trevaskis, H.D. Williams, C.W. Pouton, W.N. Charman, C.A.S. Bergström, C.J.H. Porter, 50years of oral lipid-based formulations: Provenance, progress and future perspectives, Adv Drug Deliv Rev. 101 (2016) 167–194. https://doi.org/10.1016/j.addr.2016.04.007.

[3] A. Ali Khan, J. Mudassir, N. Mohtar, Y. Darwis, Advanced drug delivery to the lymphatic system: lipid-based nanoformulations, Int J Nanomedicine. 8 (2013) 2733–2744. https://doi.org/10.2147/IJN.S41521.

[4] D. Pandita, A. Ahuja, V. Lather, B. Benjamin, T. Dutta, T. Velpandian, R.K. Khar, Development of lipid-based nanoparticles for enhancing the oral bioavailability of paclitaxel, AAPS PharmSciTech. 12 (2011) 712–722. https://doi.org/10.1208/s12249-011-9636-8.

[5] H.L. Wong, R. Bendayan, A.M. Rauth, Y. Li, X.Y. Wu, Chemotherapy with anticancer drugs encapsulated in solid lipid nanoparticles, Adv Drug Deliv Rev. 59 (2007) 491–504. https://doi.org/10.1016/j.addr.2007.04.008.

[6] G.-H. Chai, Y. Xu, S.-Q. Chen, B. Cheng, F.-Q. Hu, J. You, Y.-Z. Du, H. Yuan, Transport Mechanisms of Solid Lipid Nanoparticles across Caco-2 Cell Monolayers and their Related Cytotoxicology, ACS Appl Mater Interfaces. 8 (2016) 5929–5940. https://doi.org/10.1021/acsami.6b00821.

[7] A. Baldi, M. Chaudhary, S. Sethi, null Abhiav, R. Chandra, J. Madan, Armamentarium of nanoscaled lipid drug delivery systems customized for oral administration: In silico docking patronage, absorption phenomenon, preclinical status, clinical status and future prospects, Colloids Surf B. 170 (2018) 637–647. https://doi.org/10.1016/j.colsurfb.2018.06.061.

[8] A.R. Neves, M. Correia-da-Silva, E. Sousa, M. Pinto, Strategies to Overcome Heparins' Low Oral Bioavailability, Pharmaceuticals. 9 (2016). https://doi.org/10.3390/ph9030037.

[9] R. Paliwal, S.R. Paliwal, G.P. Agrawal, S.P. Vyas, Biomimetic solid lipid nanoparticles for oral bioavailability enhancement of low molecular weight heparin and its lipid conjugates: in vitro and in vivo evaluation, Mol Pharm. 8 (2011) 1314–1321. https://doi.org/10.1021/mp200109m.

[10] M.R. Rekha, C.P. Sharma, Oral delivery of therapeutic protein/peptide for diabetes--future perspectives, Int J Pharm. 440 (2013) 48–62. https://doi.org/10.1016/j.ijpharm.2012.03.056.

[11] A.K. Wittkowsky, Barriers to the long-term use of low-molecular weight heparins for treatment of cancer-associated thrombosis, J Thromb Haemost. 4 (2006) 2090–2091. https://doi.org/10.1111/j.1538-7836.2006.02073.x.

[12] G. Fang, B. Tang, Advanced delivery strategies facilitating oral absorption of heparins, Asian J Pharm Sci. (2020). https://doi.org/10.1016/j.ajps.2019.11.006.

[13] T.A. Al-Hilal, F. Alam, J.W. Park, K. Kim, I.C. Kwon, G.H. Ryu, Y. Byun, Prevention effect of orally active heparin conjugate on cancer-associated thrombosis, J Control Release. 195 (2014) 155–161. https://doi.org/10.1016/j.jconrel.2014.05.027.

[14] B.P. Ross, I. Toth, Gastrointestinal absorption of heparin by lipidization or coadministration with penetration enhancers, Curr Drug Deliv. 2 (2005) 277–287. https://doi.org/10.2174/1567201054367968.

[15] Y. Lee, S.K. Kim, D.Y. Lee, S. Lee, C.-Y. Kim, H.-C. Shin, H.T. Moon, Y. Byun, Efficacy of orally active chemical conjugate of low molecular weight heparin and deoxycholic acid in rats,

mice and monkeys, J Control Release. 111 (2006) 290–298. https://doi.org/10.1016/j.jconrel.2005.12.011.

[16] H. Harde, M. Das, S. Jain, Solid lipid nanoparticles: an oral bioavailability enhancer vehicle, Expert Opin Drug Deliv. 8 (2011) 1407–1424. https://doi.org/10.1517/17425247.2011.604311.

[17] E. Truzzi, C. Bongio, F. Sacchetti, E. Maretti, M. Montanari, V. Iannuccelli, E. Vismara, E. Leo, Self-Assembled Lipid Nanoparticles for Oral Delivery of Heparin-Coated Iron Oxide Nanoparticles for Theranostic Purposes, Molecules. 22 (2017) 963. https://doi.org/10.3390/molecules22060963.

[18] M.A. Mohammed, J.T.M. Syeda, K.M. Wasan, E.K. Wasan, An Overview of Chitosan Nanoparticles and Its Application in Non-Parenteral Drug Delivery, Pharmaceutics. 9 (2017). https://doi.org/10.3390/pharmaceutics9040053.

[19] Y. Jiao, N. Ubrich, M. Marchand-Arvier, C. Vigneron, M. Hoffman, T. Lecompte, P. Maincent, In vitro and in vivo evaluation of oral heparin-loaded polymeric nanoparticles in rabbits, Circulation. 105 (2002) 230–235. http://doi.org/10.1161/hc0202.101988

[20] C. Colonna, B. Conti, P. Perugini, F. Pavanetto, T. Modena, R. Dorati, P. Iadarola, I. Genta, Ex vivo evaluation of prolidase loaded chitosan nanoparticles for the enzyme replacement therapy, Eur J Pharm Biopharm. 70 (2008) 58–65. https://doi.org/10.1016/j.ejpb.2008.04.014.

[21] F. Sacchetti, C. Marraccini, D. D'Arca, M. Pelà, D. Pinetti, E. Maretti, M. Hanuskova, V. Iannuccelli, M.P. Costi, E. Leo, Enhanced anti-hyperproliferative activity of human thymidylate synthase inhibitor peptide by solid lipid nanoparticle delivery, Colloids Surf B. 136 (2015) 346–354. https://doi.org/10.1016/j.colsurfb.2015.09.040.

[22] Y.-C. Ho, F.-L. Mi, H.-W. Sung, P.-L. Kuo, Heparin-functionalized chitosan–alginate scaffolds for controlled release of growth factor, Int J Pharm. 376 (2009) 69–75. https://doi.org/10.1016/j.ijpharm.2009.04.048.

[23] J. Berger, M. Reist, J.M. Mayer, O. Felt, R. Gurny, Structure and interactions in chitosan hydrogels formed by complexation or aggregation for biomedical applications, Eur J Pharm Biopharm. 57 (2004) 35–52. https://doi.org/10.1016/S0939-6411(03)00160-7.

[24] W. Sun, S. Mao, D. Mei, T. Kissel, Self-assembled polyelectrolyte nanocomplexes between chitosan derivatives and enoxaparin, Eur J Pharm Biopharm. 69 (2008) 417–425. https://doi.org/10.1016/j.ejpb.2008.01.016.

[25] X. (Charlie) Tang, M.J. Pikal, Design of Freeze-Drying Processes for Pharmaceuticals: Practical Advice, Pharm Res. 21 (2004) 191–200. https://doi.org/10.1023/B:PHAM.0000016234.73023.75.

[26] E. Vighi, M. Montanari, M. Hanuskova, V. Iannuccelli, G. Coppi, E. Leo, Design flexibility influencing the in vitro behavior of cationic SLN as a nonviral gene vector, Int J Pharm. 440 (2013) 161–169. https://doi.org/10.1016/j.ijpharm.2012.08.055.

[27] Ü. Gönüllü, M. Üner, G. Yener, E.F. Karaman, Z. Aydoğmuş, Formulation and

characterization of solid lipid nanoparticles, nanostructured lipid carriers and nanoemulsion of lornoxicam for transdermal delivery, Acta Pharm. 65 (2015) 1–13. https://doi.org/10.1515/acph-2015-0009.

[28] P. Sundaramurthi, R. Suryanarayanan, Calorimetry and complementary techniques to characterize frozen and freeze-dried systems, Adv. Drug Deliv. Rev. 64 (2012) 384–395. https://doi.org/10.1016/j.addr.2011.12.004.

[29] M. Nasr, S. Mansour, N.D. Mortada, A.A. El Shamy, Lipospheres as Carriers for Topical Delivery of Aceclofenac: Preparation, Characterization and In Vivo Evaluation, AAPS PharmSciTech. 9 (2008) 154–162. https://doi.org/10.1208/s12249-007-9028-2.

[30] M.R. Patel, M.F. San Martin-Gonzalez, Characterization of ergocalciferol loaded solid lipid nanoparticles, J. Food Sci. 77 (2012) N8-13. https://doi.org/10.1111/j.1750-3841.2011.02517.x.

[31] P.-A. Billat, E. Roger, S. Faure, F. Lagarce, Models for drug absorption from the small intestine: where are we and where are we going?, Drug Discov. Today. 22 (2017) 761–775. https://doi.org/10.1016/j.drudis.2017.01.007.

[32] R. Joubert, J.D. Steyn, H.J. Heystek, J.H. Steenekamp, J.L. Du Preez, J.H. Hamman, In vitro oral drug permeation models: the importance of taking physiological and physico-chemical factors into consideration, Expert Opin Drug Deliv. 14 (2017) 179–187. https://doi.org/10.1080/17425247.2016.1211639.

[33] R. Gaspar, R. Duncan, Polymeric carriers: preclinical safety and the regulatory implications for design and development of polymer therapeutics, Adv Drug Deliv Rev. 61 (2009) 1220–1231. https://doi.org/10.1016/j.addr.2009.06.003.

[34] S. Rodrigues, A.M.R. da Costa, A. Grenha, Chitosan/carrageenan nanoparticles: effect of cross-linking with tripolyphosphate and charge ratios, Carbohydr Polym. 89 (2012) 282–289. https://doi.org/10.1016/j.carbpol.2012.03.010.

[35] T. Mosmann, Rapid colorimetric assay for cellular growth and survival: Application to proliferation and cytotoxicity assays, J Immunol Methods. 65 (1983) 55–63. https://doi.org/10.1016/0022-1759(83)90303-4.

[36] G. Coppi, M. Montanari, T. Rossi, M. Bondi, V. Iannuccelli, Cellular uptake and toxicity of microparticles in a perspective of polymyxin B oral administration, Int J Pharm. 385 (2010) 42–46. https://doi.org/10.1016/j.ijpharm.2009.10.026.

[37] A. Katsikari, C. Patronidou, C. Kiparissides, M. Arsenakis, Uptake and cytotoxicity of poly(d,l-lactide-co-glycolide) nanoparticles in human colon adenocarcinoma cells, Mat Sci Eng B. 165 (2009) 160–164. http://doi.org/10.1016/j.mseb.2009.09.007.

[38] S. Xiong, X. Zhao, B.C. Heng, K.W. Ng, J.S.-C. Loo, Cellular uptake of Poly-(D,L-lactide-co-glycolide) (PLGA) nanoparticles synthesized through solvent emulsion evaporation and nanoprecipitation method, Biotechnology Journal. 6 (2011) 501–508. https://doi.org/10.1002/biot.201000351.

[39] L.-L. Shi, Y. Cao, X.-Y. Zhu, J.-H. Cui, Q.-R. Cao, Optimization of process variables of zanamivir-loaded solid lipid nanoparticles and the prediction of their cellular transport in Caco-2 cell model, Int J Pharm. 478 (2015) 60–69. https://doi.org/10.1016/j.ijpharm.2014.11.017.

[40] J.D. Schulz, M.A. Gauthier, J.-C. Leroux, Improving oral drug bioavailability with polycations?, Eur J Pharm Biopharm. 97 (2015) 427–437. https://doi.org/10.1016/j.ejpb.2015.04.025.

[41] M.P. Moyer, L.A. Manzano, R.L. Merriman, J.S. Stauffer, L.R. Tanzer, NCM460, a normal human colon mucosal epithelial cell line, In Vitro Cell Dev Biol Anim. 32 (1996) 315–317. http://doi.org/ 10.1007/BF02722955.

[42] A. Dalpiaz, V. Ferretti, V. Bertolasi, B. Pavan, A. Monari, M. Pastore, From Physical Mixtures to Co-Crystals: How the Coformers Can Modify Solubility and Biological Activity of Carbamazepine, Mol Pharm. 15 (2018) 268–278. https://doi.org/10.1021/acs.molpharmaceut.7b00899.

[43] V. Ferretti, A. Dalpiaz, V. Bertolasi, L. Ferraro, S. Beggiato, F. Spizzo, E. Spisni, B. Pavan, Indomethacin Co-Crystals and Their Parent Mixtures: Does the Intestinal Barrier Recognize Them Differently?, Mol Pharm. 12 (2015) 1501–1511. https://doi.org/10.1021/mp500826y.

[44] Z.-H. Liu, T.-Y. Shen, P. Zhang, Y.-L. Ma, M.P. Moyer, H.-L. Qin, Protective effects of Lactobacillus plantarum against epithelial barrier dysfunction of human colon cell line NCM460, World J Gastroenterol. 16 (2010) 5759–5765. http://doi.org/ 10.3748/wjg.v16.i45.5759.

[45] J. Sahi, S.G. Nataraja, T.J. Layden, J.L. Goldstein, M.P. Moyer, M.C. Rao, Cl- transport in an immortalized human epithelial cell line (NCM460) derived from the normal transverse colon, Am J Physiol. 275 (1998) C1048-1057. https://doi.org/10.1152/ajpcell.1998.275.4.C1048.

[46] B. Rothen-Rutishauser, A. Braun, M. Günthert, H. Wunderli-Allenspach, Formation of multilayers in the caco-2 cell culture model: a confocal laser scanning microscopy study, Pharm Res. 17 (2000) 460–465. http://doi.org/ 10.1023/A:1007585105753.

[47] V. Gupta, B.H. Hwang, N. Doshi, S. Mitragotri, A permeation enhancer for increasing transport of therapeutic macromolecules across the intestine, J Control Release. 172 (2013) 541–549. https://doi.org/10.1016/j.jconrel.2013.05.002.

[48] A. Beloqui, A. des Rieux, V. Préat, Mechanisms of transport of polymeric and lipidic nanoparticles across the intestinal barrier, Adv Drug Deliv Rev. 106 (2016) 242–255. https://doi.org/10.1016/j.addr.2016.04.014.

[49] A. Akbari, A. Lavasanifar, J. Wu, Interaction of cruciferin-based nanoparticles with Caco-2 cells and Caco-2/HT29-MTX co-cultures, Acta Biomaterialia. 64 (2017) 249–258. https://doi.org/10.1016/j.actbio.2017.10.017.

[50] H. Hillaireau, P. Couvreur, Nanocarriers' entry into the cell: relevance to drug delivery, Cell. Mol. Life Sci. 66 (2009) 2873–2896. https://doi.org/10.1007/s00018-009-0053-z.

LEGEND TO FIGURES

Fig. 1 FTIR spectra of chitosan **(A)**, heparin **(B)**, and PEC **(C)**.

Fig. 2 (A) AFM image of PEC, freeze-dried H-SLN and PEC-SLN**; (B)** Cumulative percentage release of heparin from PEC-SLN, H-SLN and naked PEC at different pH conditions.

Fig. 3 SLN cytotoxicity on CaCo-2 cell line: empty-SLN and PEC-SLN samples at different doses (0.2, 0.4, 0.8, and 1.2 mg/mL) and growing incubation time (a) 4h, (b) 6h, (c) 12h; (d) naked PEC cytotoxicity at 4, 6 and 12h incubation time (dotted line as the control).

Fig. 4 Cytometric analysis of (a) Nile Red labeled empty-SLN and PEC-SLN at 0.2, 0.4, 0.8 and 1.2 mg/mL and (b) FITC labeled PEC at 15, 30, 60 and 90 µg/mL on CaCo-2 cell line expressed as cell fluorescence percentage in function of the incubation time (4, 6 and 12h).

Fig. 5 Confocal microscopy images of CaCo-2 cells after nuclei staining (blue) and 4h treatment with (a) PEC-SLN labeled with Nile Red and (b) naked PEC labeled with FITC.

Fig. 6 (A) Effects of empty-SLN, PEC-SLN at 0.4 mg/mL and naked PEC at 30 µg/mL on the transepithelial electrical resistance (TEER) values of NCM460 cell monolayers after 4h treatment. Data are reported as percentages of the control values obtained at the time point 0h. **(B)** Confocal images of NCM460 cell monolayers after 4h incubation with 0.4 mg/mL of PEC-SLN labeled with Nile Red. Cell nuclei were stained with Hoechst (blue fluorescence, a) and SLN were labeled with Nile Red (red fluorescence, b). The image (c) reported blue and red fluorescence overlapped.

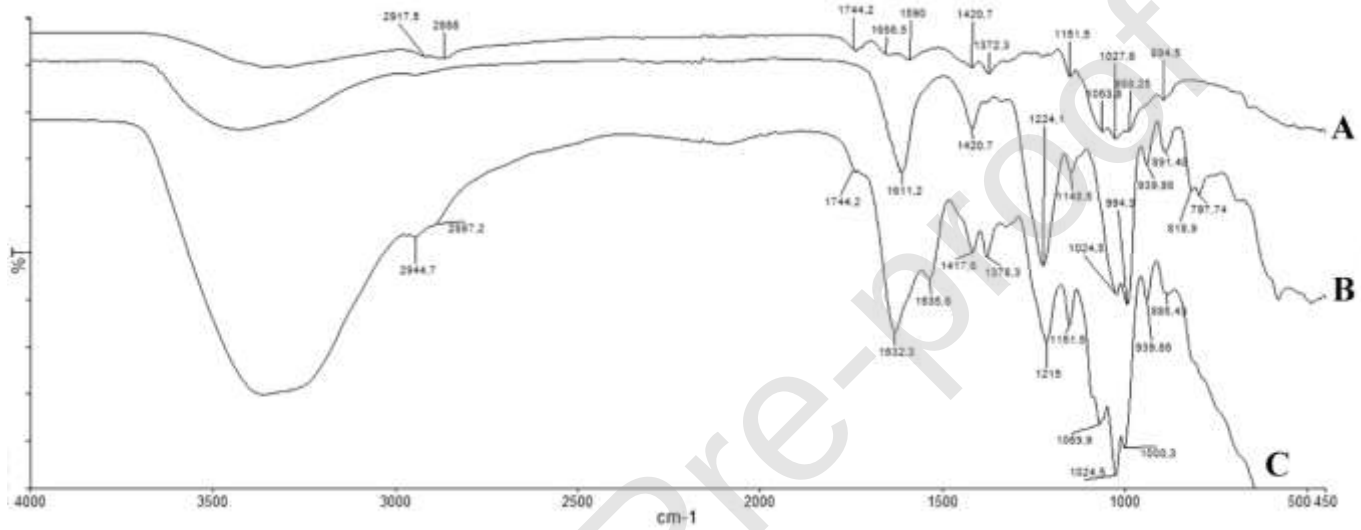

Figure 1

A

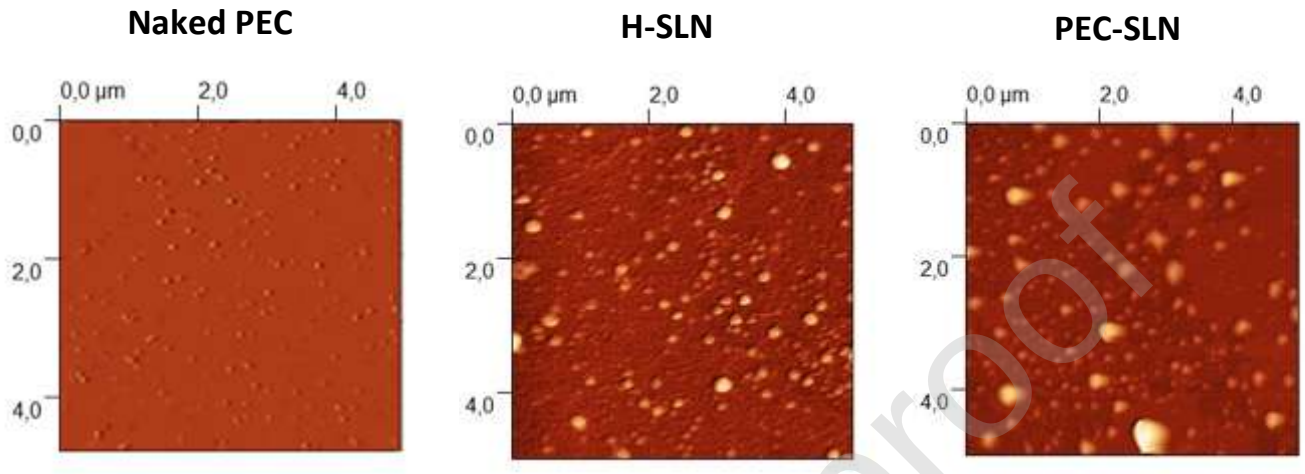

B

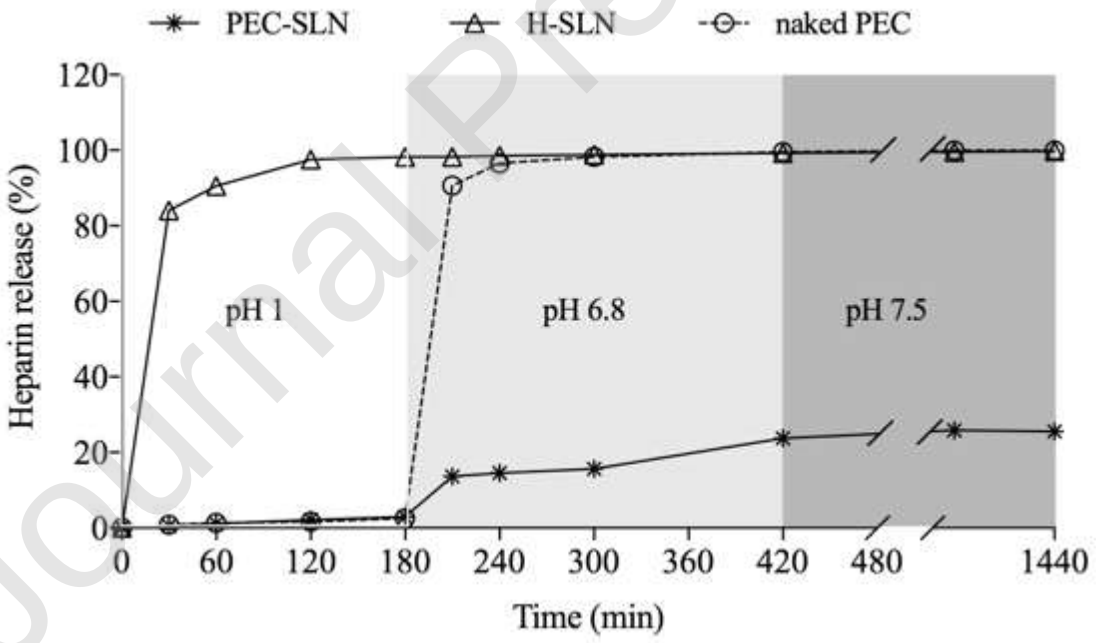

Figure 2

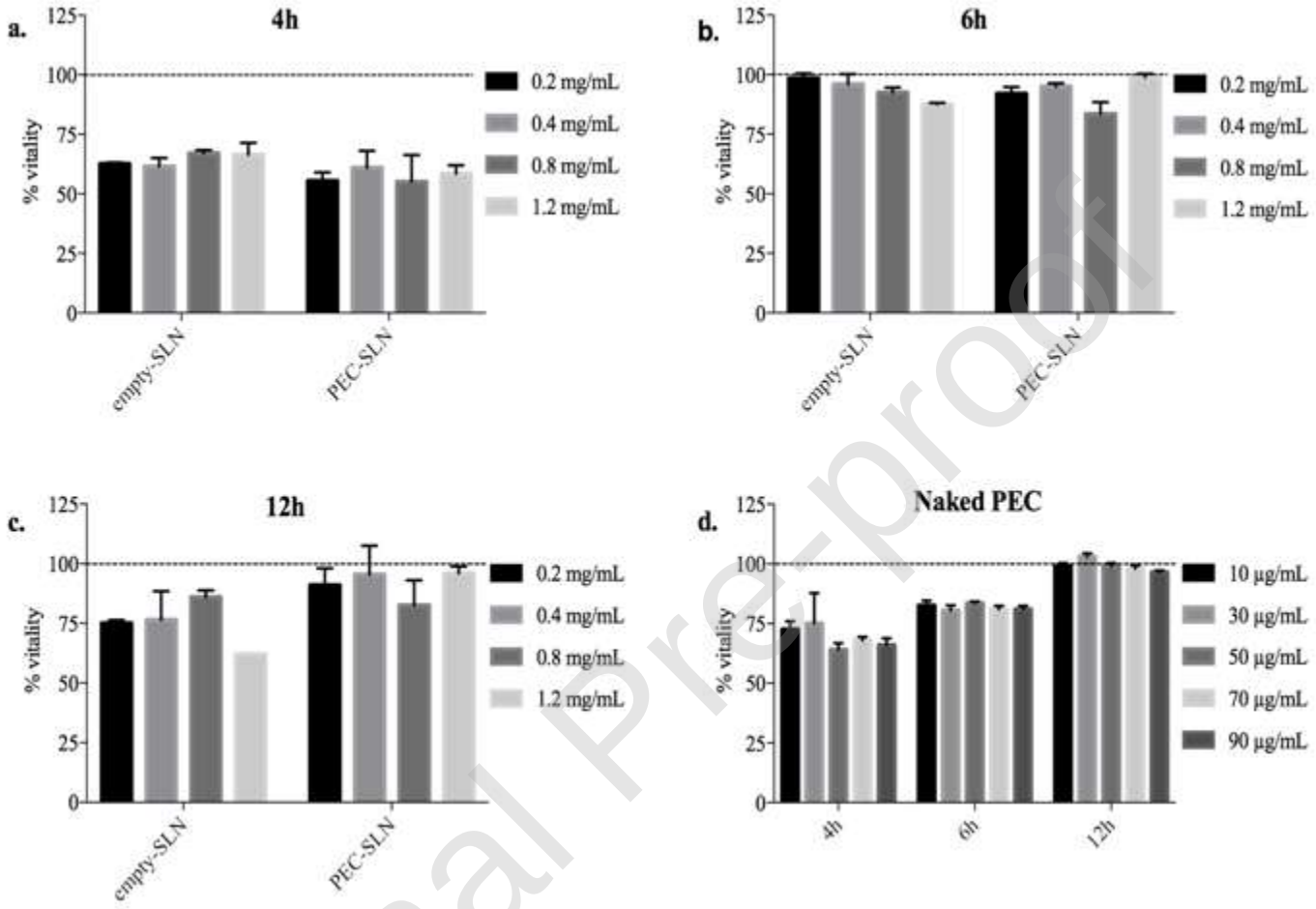

Figure 3

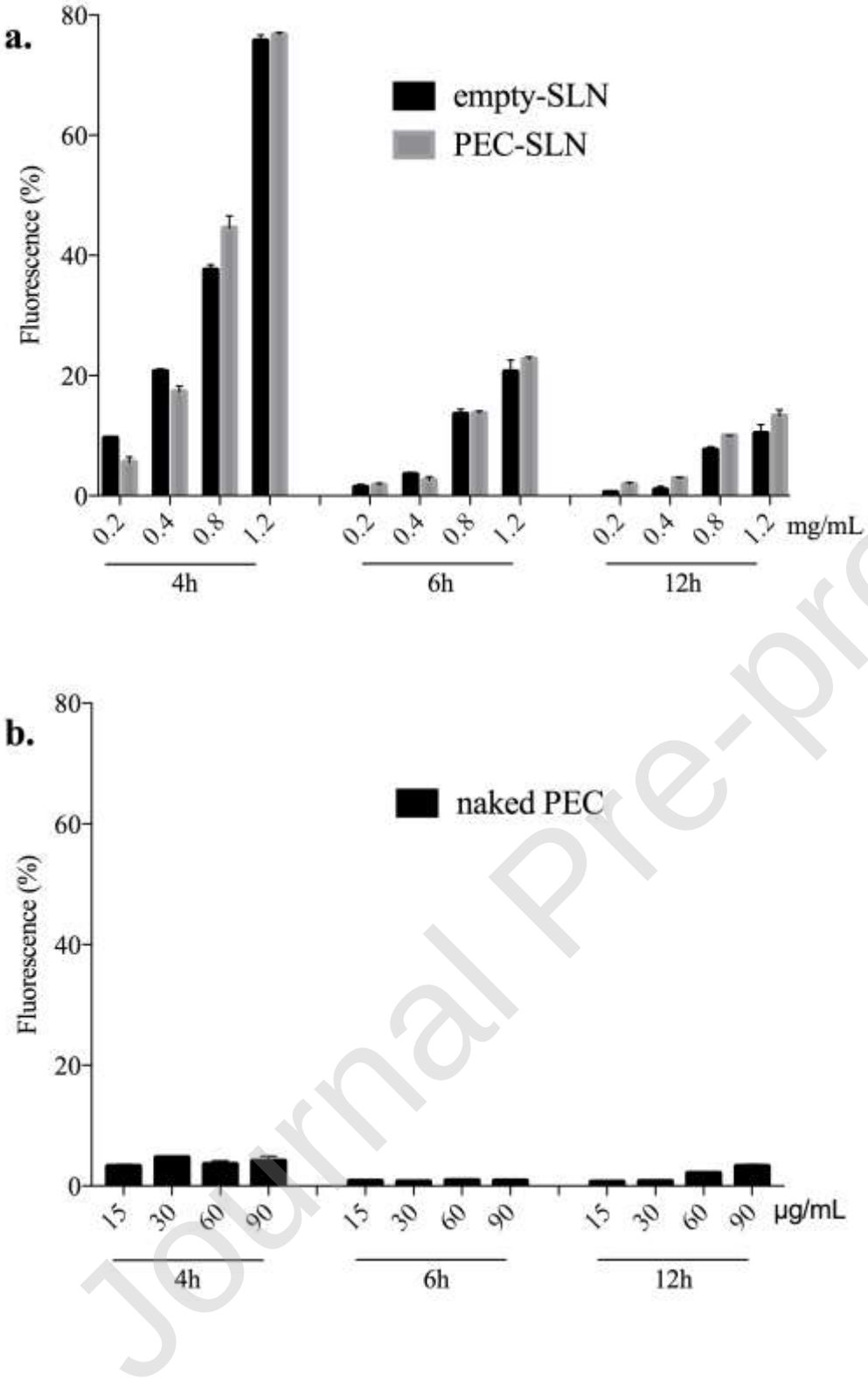

Figure 4

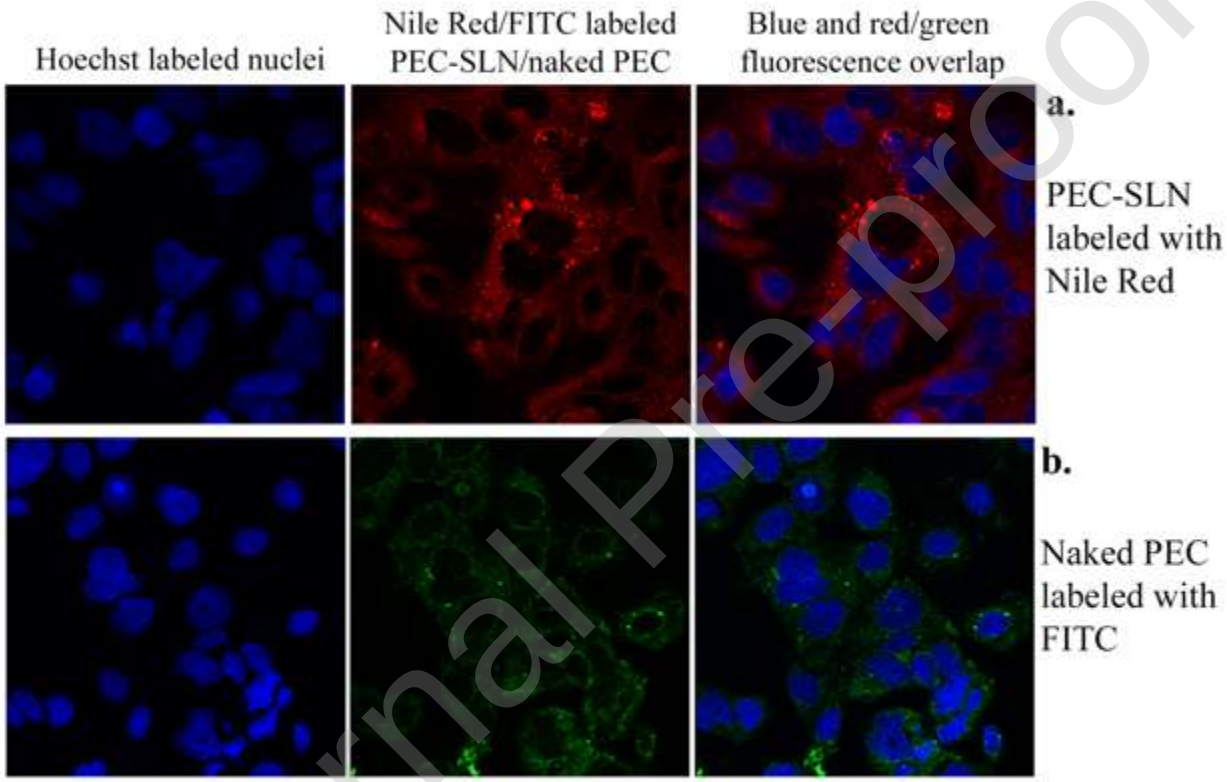

Figure 5

A

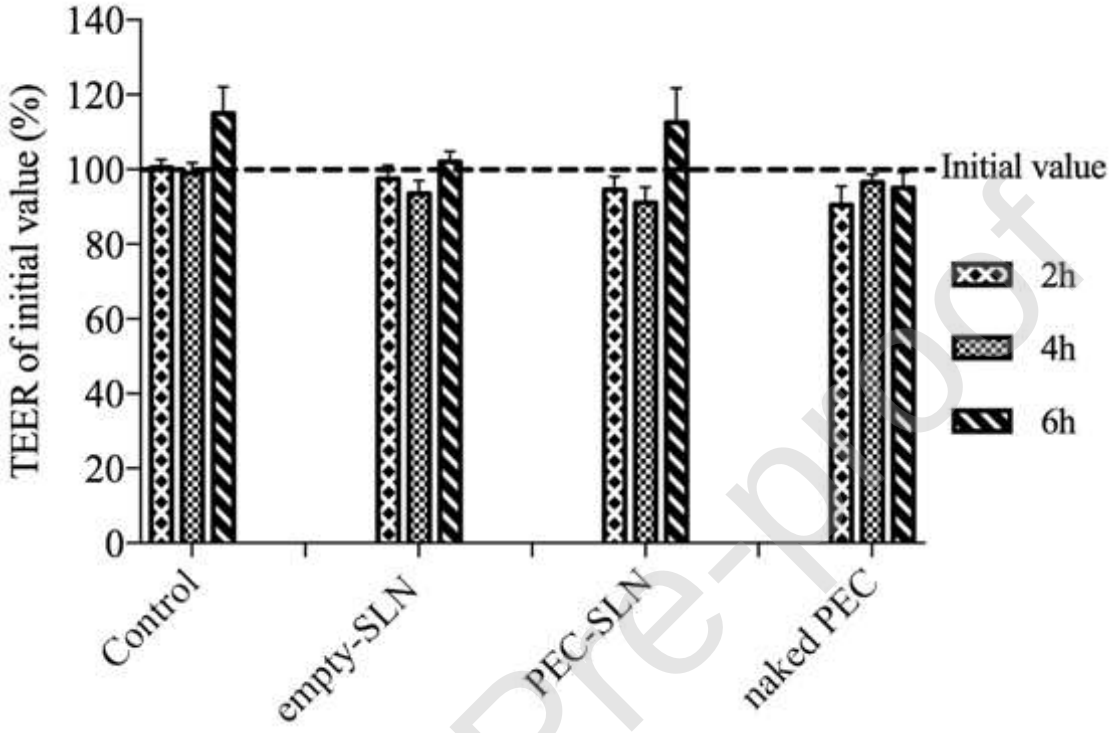

B

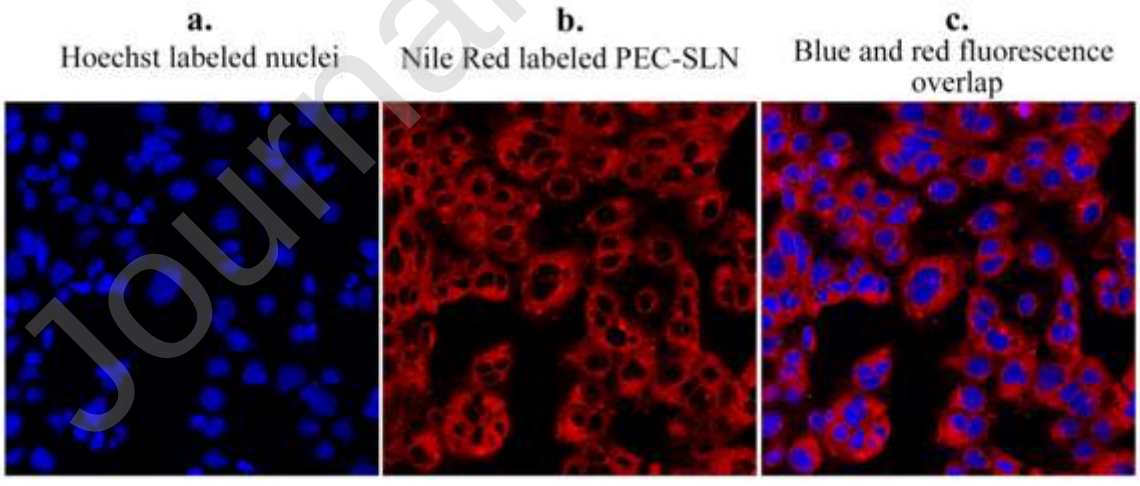

Figure 6

Table I Size and zeta potential of PEC measured at different pH conditions, mean ± SD (n = 3).

pH medium	Size (Z average, nm) (PDI)	zeta potential (mV)
pH 1.0	390 ± 40 (0.313 ± 0.071)	+22.5 ± 2.7
pH 3.0	295 ± 75 (0.213 ± 0.047)	+24.3 ± 4.3
pH 5.5	171 ± 49 (0.242 ± 0.024)	+20.1 ± 6.2
pH 6.8	597 ± 49 (0.306 ± 0.092)	+27.1 ± 3.3
pH 7.4	Macroscopic aggregates	
pH 9.2	Macroscopic aggregates	

Table II Physicochemical properties (size, PDI and zeta potential) of fresh and freeze-dried SLN. Results denote mean ± SD (n = 3).

		Size (Z average, nm)	PDI	Zeta Potential (mV)
Fresh samples	**empty-SLN**	201.3± 9.7	0.280	-23.0±4.7
	H-SLN	250.3± 8.2	0.296	-21.2±4.5
	PEC-SLN	347.8± 9.4	0.231	-10.3±4.9
Freeze-dried samples	**empty-SLN**	258.8 ± 10.2	0.358	-25.1 ± 4.4
	H-SLN	271.2 ± 9.1	0.293	-22.3 ± 4.3
	PEC-SLN	372.9± 12.4	0.419	-17.1 ± 5.4

Table III Tm (melting temperature) and ΔHm (melting enthalpy) values for lipid component recorded by DSC analysis.

Sample	T_m (°C)	ΔH_m (J/g)

Pre-heated Compritol	74.06	128.91
Pre-heated physical mixture	75.65	124.64
Empty-SLN	71.06	69.54
H-SLN	70.93	62.93
PEC-SLN	70.74	53.76

Table IV Parameters related with the encapsulation of heparin and PEC in SLN, mean ± SD.

	UNPURIFIED FRESH SUSPENSION			**PURIFIED AND FREEZE-DRIED SAMPLES**	
	Initial heparin (mg)	**Total heparin in SLN suspension (%)**	**Total heparin in SLN suspension (mg)**	**Drug loading (mg/100 mg)**	**Encapsulation efficiency (%)**
H-SLN	7	99.1 ± 0.3	6.9 ± 0.4	3.8 ± 0.8	55.1 ± 2.7
PEC-SLN	7.6 ± 0.3	93.4 ± 0.5	7.1 ± 0.2	3.1 ± 0.6	43.7 ± 1.9